



Experimental investigation of residual stress distribution on girth welds fabricated at proximity using neutron diffraction technique

Sachin Bhardwaj¹ · R. M. Chandima Ratnayake¹ · Efthymios Polatidis² · Jan Capek²

Received: 7 April 2022 / Accepted: 17 June 2022
© The Author(s) 2022

Abstract

Maintaining minimum distance between repair and existing welds often becomes impractical due to the presence of compact layouts, original welds of branches, nozzles, etc. on offshore structural elements, pipelines, and piping. Although some international codes and standards provide criteria for maintaining a minimum distance between proximity welds, most of them lack technical justification in relation to their effect on the structural integrity of welded components. The development of residual stresses has a significant effect (i.e., a negative effect on tensile stresses and a positive effect on compressive stresses) on the integrity of the welds fabricated at proximity. Hence, it is important to investigate the residual stress distribution on welds fabricated at proximity, especially at a distance away from the weld toe. This study presents findings on the characterization of residual stresses by neutron diffraction at the proximity region between two girth welds. The two welds were fabricated at proximity, using two different welding procedure specifications and at three different distances, on a structural steel pipe, grade S355. The three different welding distances between weld toes were maintained at 5, 10, and 15 mm respectively. The neutron diffraction-based residual stress distributions were investigated at the POLDI neutron instrument at the Swiss spallation source SINQ in Switzerland. The axial, hoop, and radial components of the residual stresses were experimentally investigated between proximity welds. The findings revealed that residual axial stresses at a 5-mm proximity distance were increased beyond the yield strength of the structural steel, grade S355. The findings of this study enable practitioners to take remedial actions to minimize the residual stresses developed in girth welds fabricated at proximity. Also, the findings enable us to derive technical justification for maintaining a minimum distance and developing welding procedure for welds fabricated at proximity.

Keywords Residual stress · Neutron diffraction · Proximity welds · Repair welds

1 Introduction

Welds placed at proximity have always been found to be a subject of debate among fabricators, inspectors, and contractors. International fabrication codes and standards often fail to provide technical justification for maintaining a minimum distance between proximity welds [1, 2]. During the replacement/repair fabrication procedures of tubular structures, the standards provide no guidelines regarding maintaining

minimum distances between original and repair welds [3]. Proximity welds' placement should be based on practical experience, and shorter distances may need to be proven with respect to both impact on stress concentration factors (SCFs) and welding residual stresses' (WRS) estimation, as mentioned in code [4], which is used for offshore wind turbines' assessment. Detailed evaluation of this criteria has been performed in the past by the authors [3] for proximity weld configurations found in various structural fabrication and repair codes [3]. The challenges of welding repair joints on or at proximity to existing welds, leading to the development of harmful tensile WRS development, have been well documented by [5–7]. These can cause failures due to stress corrosion cracking at a distance away from weld in welded austenitic steel piping. Imperfections in welds, coupled with high tensile WRS under high cyclic loading conditions, are well known for causing major weld failures in high restraint

✉ R. M. Chandima Ratnayake
chandima.ratnayake@uis.no

¹ Department of Mechanical and Structural Engineering and Materials Science, University of Stavanger, N-4036 Stavanger, Norway

² Laboratory for Neutron Scattering and Imaging, Paul Scherrer Institute, CH-5232 Villigen PSI, Switzerland

proximity welds of tubular braces and offshore jackets [8], floating production storage and offloading (FPSOs) [9], and tubular bridge structures' truss welds [10]. Hence, it is important to estimate the WRS distribution around the weld toe and proximity regions.

WRS characterization around the weld toe region has always been considered a subject of interest for designers, manufacturers, and integrity engineers, as harmful tensile residual stresses have been found to accelerate crack propagation, in contrast to beneficial compressive stresses in welded joints [11]. Accurate estimation of stress intensity factors due to residual stresses can further help in better predicting the remaining fatigue life of welded joints, while using fracture mechanics procedures for welded joints [12]. In the various defect assessment procedures of fitness for service codes (FFS) like BS 7910 [13], API-579 [14], and R6 [15], WRS profiles for distances away from the weld toe (WT) [16], and welds placed at close proximity, like critical offshore brace joints, piping welds etc., are not available [1], often leading to conservative assessments in FFS procedures. In addition to the formation of deleterious tensile residual stresses between proximity welds, heat input, weld sequence, and restraint conditions in the employed welding process play a vital role in developing yield level residual stress at the weld center and proximity regions.

The estimation of tensile residual stresses between proximity welds, fabricated with similar welding processes on a butt-welded plate, have previously been reported by [17], by the use of techniques like X-ray diffraction and incremental center-hole drilling. Similar findings, developed at proximity regions between proximity K-welded tubular joints, by the use of neutron diffraction and X-ray diffraction (XRD) techniques, have been reported by [18]. However, in both the cases, through thickness level, residual stresses were not measured at proximity region developed between adjacent weld toes, due to depth measurement limitation of XRD technique and use of neutron diffraction technique at weld toe location only. Changes in mechanical properties of proximity welds like fatigue life, hardness, tensile, and impact tests on butt-welded plate and partial penetration K-welded joints of tubular offshore joints, respectively, have been reported by authors [2, 19] and [20] in the past. Mechanical test results and welding qualification for repair proximity welds, fabricated on a pipe, have previously been presented by authors [21], indicating the development of high hardness and low energy values at proximity regions. However, in repair/replacement welds, fabrication with two different welding processes at different proximity distances, leading to the development of harmful or beneficial WRS profiles, needs to be investigated, for which no reported experimental study was found in open literature.

Therefore, the aim of the current study is to investigate the effect of proximity welds on WRS profiles developed

between adjacent weld toes, fabricated with two different welding processes on a structural steel pipe of grade S355. The neutron diffraction (ND) technique was employed for characterizing the residual stresses between proximity welds on a large tubular welded mockup, with the use of the time of flight neutron diffractometer (POLDI, SINQ) at the Paul Scherrer Institute (PSI), in Switzerland. The remainder of the paper is structured as follows: Sect. 2 describes the experimental methodology, followed by the results and discussion. Subsequently, in Sect. 4, a conclusion is drawn.

2 Experimental procedure

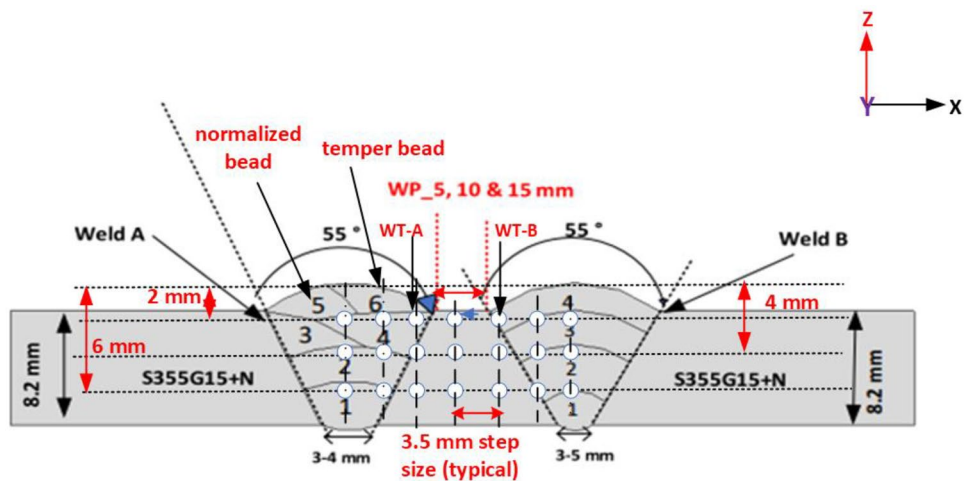
2.1 Large, welded mockup samples

Proximity multi-pass girth welds were fabricated on structural steel-grade EN 10,225–09 S355G14+N seamless pipe, generally used in the fabrication of offshore structural members [8], with dimensions of 219.1 mm outside diameter and 8.18 mm thickness. Initially, weld A was fabricated as a single weld on a pipe Sect. 700 mm long, welded with tungsten inert gas (TIG), a semi-automatic welding process, and, subsequently, a vee groove for weld B was machine cut. Lastly, weld B was welded with metal active gas (MAG), a semi-automatic method for root pass, and Flux cored arc welding (FCAW), a semi-automatic method for the remaining passes after the completion of weld A. Weld proximity (WP) distances of 5 mm, 10 mm, and 15 mm were maintained between adjacent weld toes, as shown in Fig. 1 schematic.

As discussed previously, to simulate the practical situation of repair or replacement procedures, weld B was welded with different and faster welding processes like MAG and FCAW, in contrast to weld A, which was welded with TIG, which is a more factory-controlled welding process. Complete details about the material properties, fabrication process, welding procedure qualification record (WPQR), filler wire, digital weld log data, and mechanical testing results can be found in the authors' previous work [21]. All necessary NDTs, e.g., radiography & destructive testing (DT), e.g., tensile, Charpy, hardness, and bend tests to qualify WPQR for proximity welds were performed on all samples, as per the criteria mentioned in ISO EN15614-1 [22].

ISO EN15614-1 [22] code was used for the qualification of WPQR and adopted in this project catering for the Norwegian continental shelf (NCS) and offshore welded tubular structures used in oil exploration and the processing industry. ISO EN15614-1 is a widely accepted code for welding qualification around the world. Welding was performed under controlled conditions after optimizing the welding parameters found in [21] as per pre-qualified welding procedure specification (WPS) adopted from reputable industrial partners. Three samples from each proximity distance of 5,

Fig. 1 Schematic of proximity welds at 5, 10, and 15 mm distances and neutron diffraction measurement points



10, and 15 mm were finally fabricated and characterized by neutron diffraction, as explained in following section.

2.2 Neutron diffraction measurements

Neutron diffraction is a nondestructive technique (NDT) that is capable of measuring residual strains in the bulk of multi-pass welds and most polycrystalline metal and alloys [23]. Neutron diffraction measurements were performed at the pulse overlap diffractometer (POLDI), located at the Swiss Spallation Source, SINQ, at the Paul Scherrer Institute in Switzerland [24] as shown in Fig. 2 schematic. POLDI is a time-of-flight (ToF) thermal neutron diffractometer, well suited to measuring spatially resolved residual stresses in engineering components. A ToF instrument like POLDI has the advantage of capturing several diffraction peaks, which is essential for the analysis of stress in strongly textured

materials. The obtained data were fitted using open source software Mantid [25]

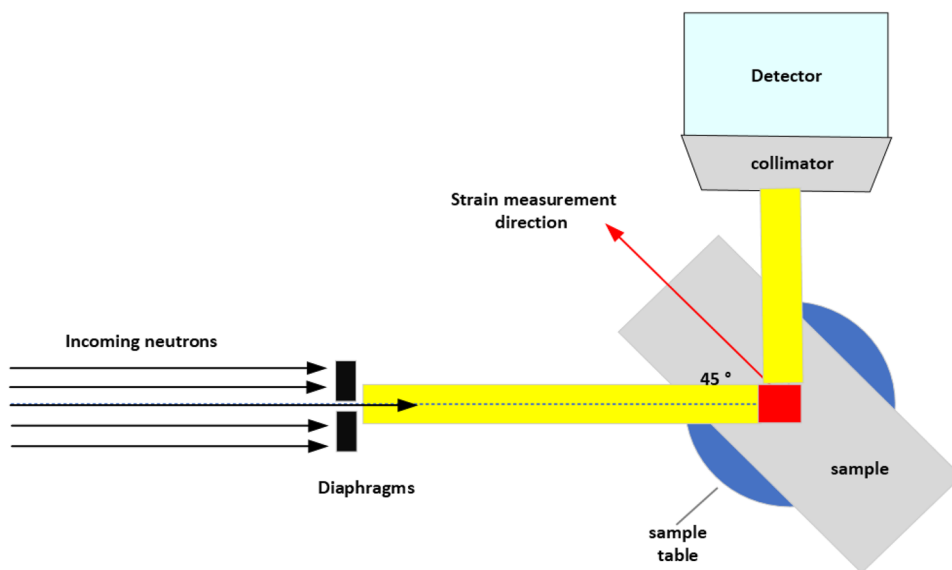
Strain can be calculated by measuring a change in the atomic lattice spacing $d_{hkl} \sim d$, acting under stress when compared with stress-free spacing d_0 , as per Eq. (1). Miller indices (hkl) are parallel to the crystallographic planes of the material, and its lattice spacing d can be found by Bragg’s law, as mentioned in Eq. (2).

$$\epsilon = \frac{d - d_0}{d_0} \tag{1}$$

$$n\lambda = 2d\sin\theta \tag{2}$$

The axial (perpendicular to weld), hoop (parallel to weld), and radial (through thickness) strain components were measured using the 211 diffraction peak for the body-centered

Fig. 2 Schematic of POLDI at PSI, Switzerland, adapted from [24]



cubic (BCC) crystal structure of the S355 alloy, as recommended in ISO21432:2019 standard [26]. Residual stresses can be calculated using generalized Hooke’s law [26], as per Eqs. (3), (4), and (5) using the plane-specific elastic constants $E_{211} = 220000MPa$ and Poisson’s ratio $\nu_{211} = 0.28$ [10]

$$\sigma_x = \frac{E}{(1 + \mu)(1 - 2\mu)} [(1 - \mu)\epsilon_x + \mu(\epsilon_y + \epsilon_z)] \quad (3)$$

$$\sigma_y = \frac{E}{(1 + \mu)(1 - 2\mu)} [(1 - \mu)\epsilon_y + \mu(\epsilon_x + \epsilon_z)] \quad (4)$$

$$\sigma_z = \frac{E}{(1 + \mu)(1 - 2\mu)} [(1 - \mu)\epsilon_z + \mu(\epsilon_y + \epsilon_x)] \quad (5)$$

where x, y, z are 3 principal orthogonal directions corresponding to either axial, or hoop or radial directions in the sample coordinate system.

Measurement points started as a line scan from the center of weld A, along the case-specific proximity distance, moving towards the center of weld B, with a step size of 3.5 mm and a gauge volume of $3.8 \times 3.8 \times 3.8 \text{ mm}^3$, as illustrated in Fig. 1. The line scan area was selected away from the weld start and stop positions and was performed in three different depths, i.e., 2, 4, and 6 mm from the top of the weld cap into the thickness, as shown in Fig. 1. As shown in Fig. 3, neutron beam exit paths through window cuts are illustrated for hoop and axial measurements. The beam is incident at 45° to the measurement location and exits at an angle of 90° . Appropriately sized window cuts were machined with a size of $200 \times 50 \text{ mm}$ at 90° to the line scan area, i.e., the proximity region from the center of weld A to B, during hoop stress measurements. A similar size window cut was also made at 180° to the line scan area, 150 mm away from the pipe center, for the beam exit during axial stress measurements. This was done to avoid the neutron attenuation by the beam

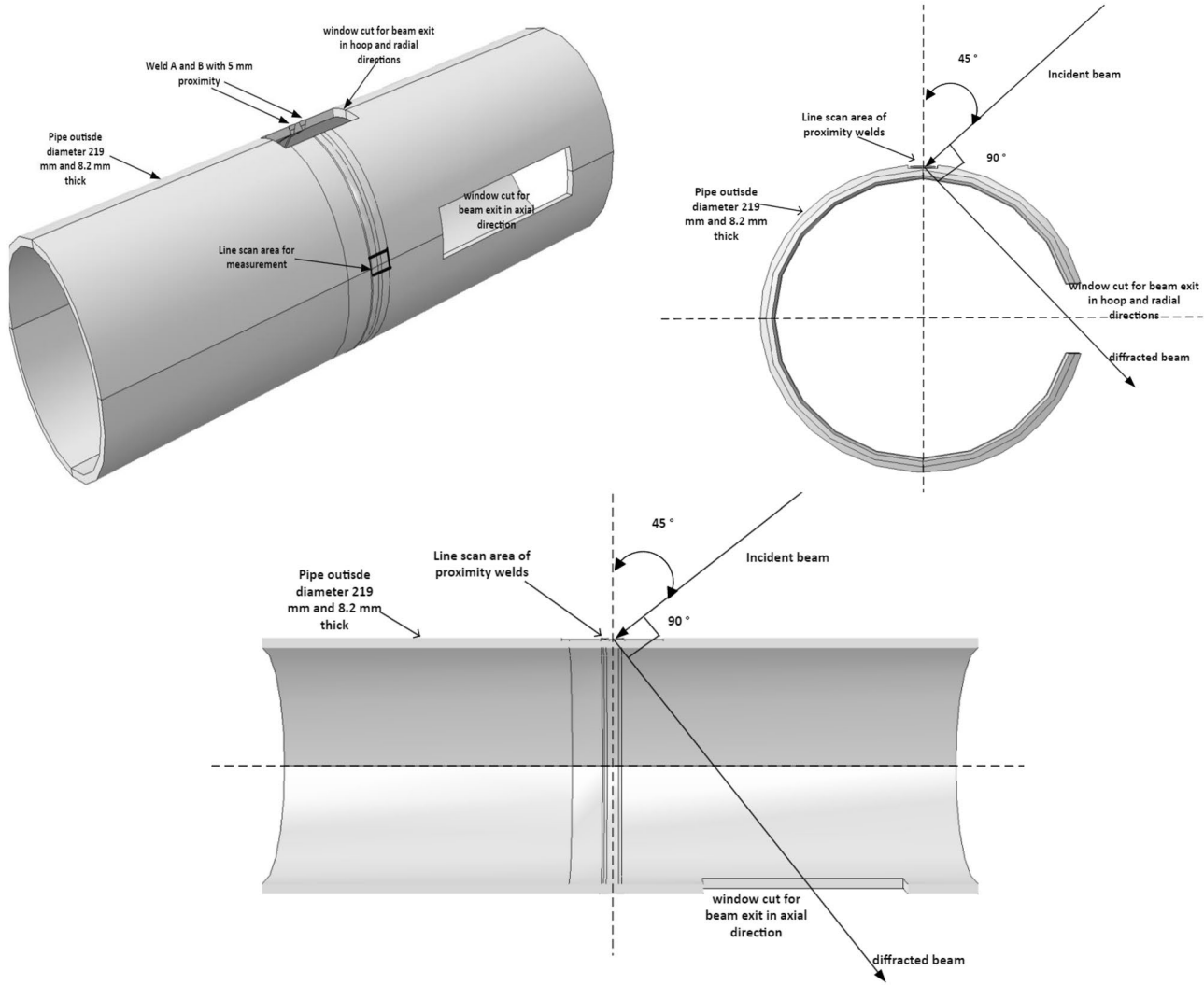


Fig. 3 Neutron beam exit path schematic in hoop and axial directions

passing through the tube wall for the second time in either the incident or diffracted direction.

2.3 Stress-free reference samples for “ d_0 ” measurements

A stress-free location for d_0 measurements was chosen, starting from center of weld A towards B, to take account of any chemical variation taking place due to the use of different welding processes, as shown in Fig. 4. The d_0 samples were cut by electrical discharge machining (EDM), as thin slices of 1 mm thickness, to achieve a stress-free state, as previously reported by [18, 27] for tubular welded structures. The reference d_0 measurement was undertaken at mid-thickness of d_0 samples, i.e., at 4 mm depth from the top, starting from the center of weld A towards B, at five different locations, i.e., the center of weld A, weld toe A (WT-A), proximity area, weld toe B (WT-B), and center of weld B, as shown in Fig. 4. It was also decided to anneal d_0 samples for 2 h at 1066 °C, a common stress-relieving procedure [28], and perform measurements at the same locations as the EDM cuts for various proximity distances. This was done to take account of any uncertainty observed when taking measurements with two different techniques. It was observed that there is very small variation (i.e., below variation resulting in 100 μe uncertainty) within the line scan of the d_0 samples, and therefore a single d_0 value was used throughout the analysis, i.e., a value of 1.1738 Å.

Fig. 5 Representative neutron diffraction pattern: experimental data (green circles), the fit profile (solid black line), and the residuals (solid grey line). The inset represents a zoom of the 211 diffraction peak

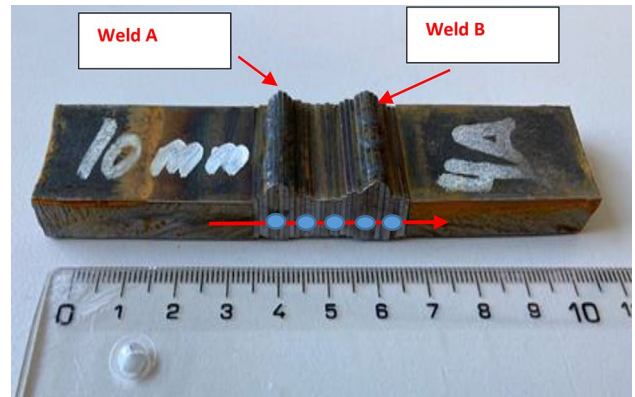
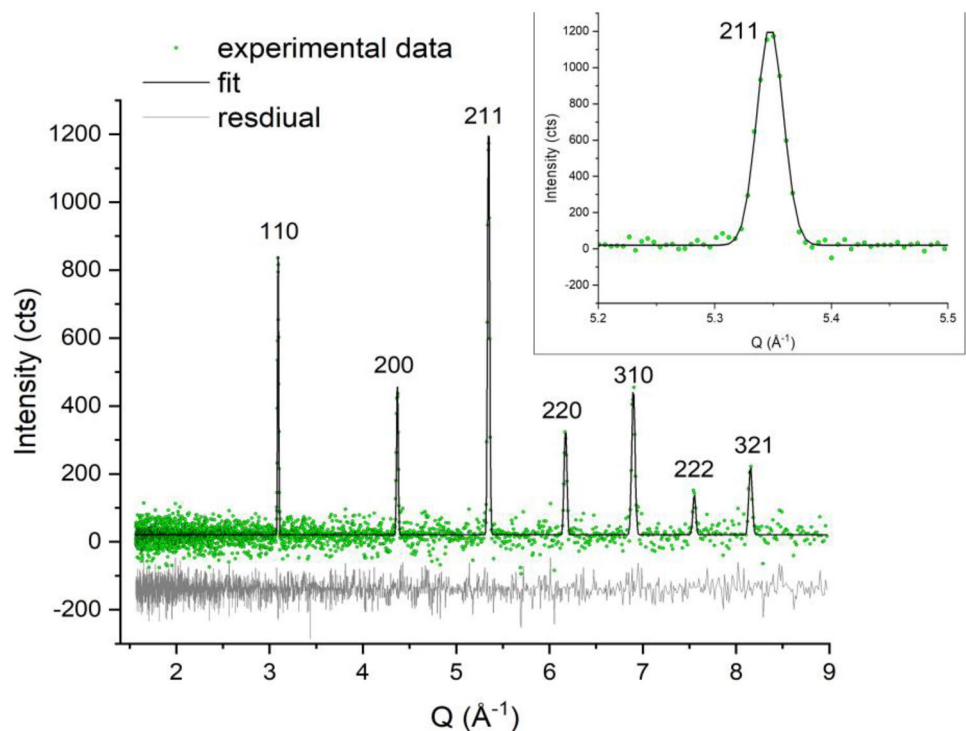


Fig. 4 Stress-free reference samples for d_0 measurement at specified locations

3 Results and discussion

The diffraction spectrum, representing the intensity versus the scattering angle for all diffraction peaks are shown in Fig. 5. As explained in Sect. 2.2, the (211) peak intensity used for strain calculation is also highlighted for measured samples. The results of line scan are presented in Figs. 6, 7, and 8, in axial (perpendicular to the weld direction), hoop (parallel to the weld direction), and radial (into the thickness) principal directions, respectively, when measured at

2, 4, and 6 mm depths from top of the weld cap into the thickness, by neutron diffraction technique.

3.1 Axial residual stress: transverse to weld direction

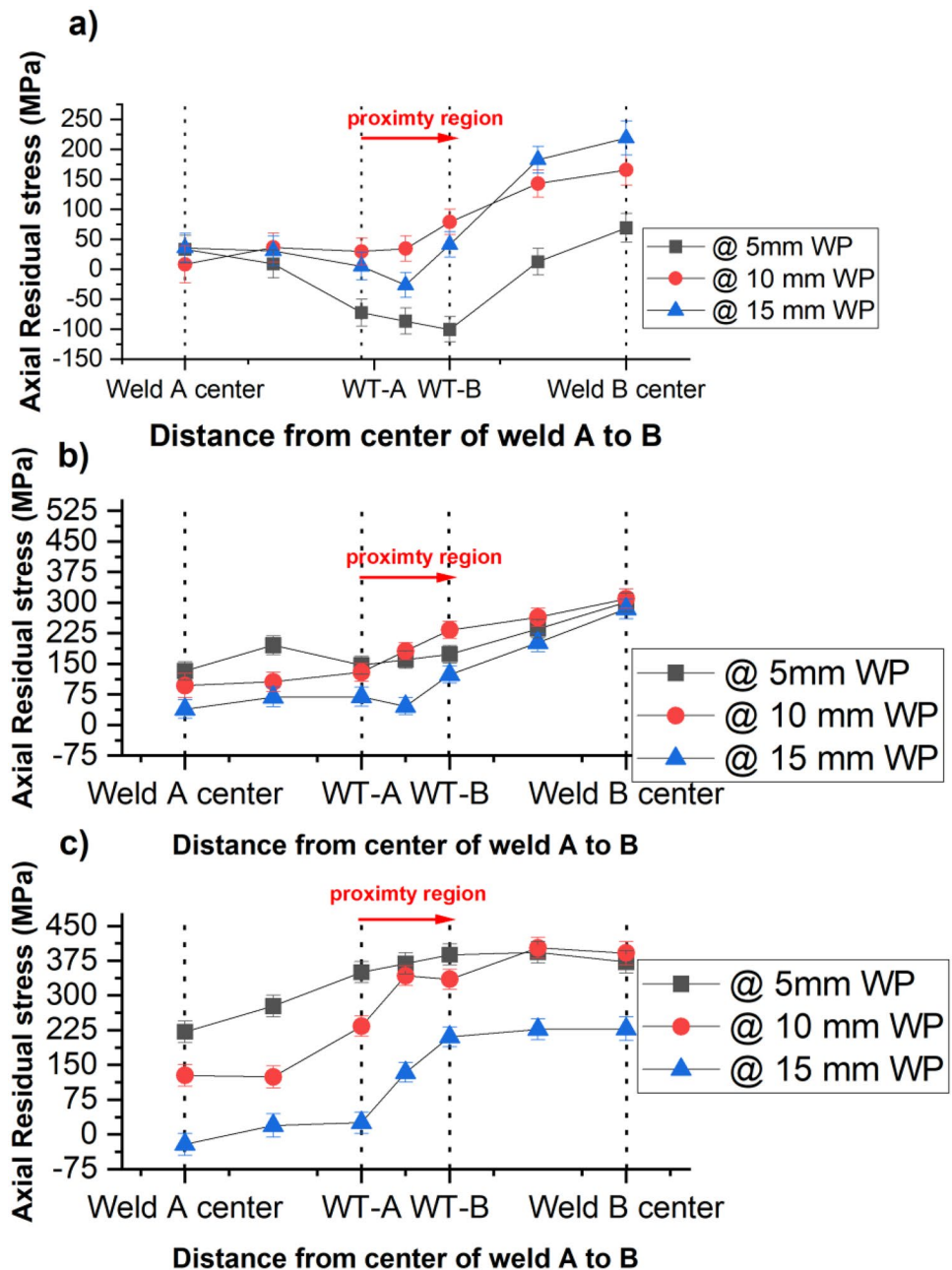
Axial residual stresses (perpendicular to weld direction–transverse) become more important in girth welds’ assessment of piping, pipelines, and tubular structures, due to the dominant axial loading conditions [29]. As shown in Fig. 6, axial residual stress for WP 5, 10, and 15 mm distances are presented when measured at different depths (2, 4, and

6 mm) from the top of the weld cap to the bottom, starting from the center of weld A towards B.

3.1.1 Stress at proximity regions

At 2 mm depth from the top of the weld cap into the thickness, due to the closest interaction between the adjacent weld cap toes, i.e., 5 mm, and maximum tempering effect due to the adjacent placement of weld B, axial residual stresses observed at the proximity region are low in magnitude, with a value of compressive 86 ± 18 MPa, as shown in Fig. 6a. At 2 mm depths from the top of the weld cap into the thickness

Fig. 6 Axial residual stress for WP_5mm, WP_10mm, WP_15mm proximity distances at a) 2 mm (cap) b) 4 mm (mid thickness) c) 6 mm depth (root), level respectively



for 10 and 15 mm weld proximity distances, the axial stress values are seen to become tensile, in contrast to the 5 mm proximity distance, due to the decreasing effect of tempering, present between adjacent weld caps.

At the closest WP distance, i.e., at 5 mm, the effect on axial residual stress can be seen to be most dominant at 4 and 6 mm depths, when compared with 10 and 15 mm proximity distances, as shown in Fig. 6b and c. This can be attributed to the following reasons: maximum restraint effect caused by adjacent weld B, higher rate of cooling of weld B (FCAW – low heat input process), and welding sequence, as weld B was fabricated after the completion of weld A. The closest proximity distance of 5 mm leads to an increase in the magnitude of axial tensile residual stresses from 160 ± 18 MPa to 368 ± 18 MPa, when compared at 4 and 6 mm depths, respectively. The highest value of tensile axial stress of 368 ± 18 MPa, measured for 5 mm proximity distance at 6 mm depth from the top, is found to be higher than the yield strength of the parent material S355 used in this study, i.e., 355 MPa, which can be detrimental for the weld integrity, when superimposed with axial cyclic loadings, as observed by [18] from the neutron diffraction results of K-tubular proximity welds. Stresses, measured at the proximity region of 10 mm distance, at 4 and 6 mm depths, show values increasing from 181 MPa to 342 ± 18 MPa, respectively, in contrast to the 15 mm proximity distance, where values increase from 46 ± 18 MPa to 133 ± 18 MPa, respectively. As 15 mm is the maximum proximity distance used in this current study, the stress values observed between welds are found to be lower when compared with 5 and 10 mm proximity cases.

As reported by [30, 31], repair welds tend to produce high tensile residual stress, due to the local effect developed at the proximity regions or around the weld toes, causing high restraint and stress zones. The current study of fabricating repair weld B adjacent to original weld A also creates the situation of high restraint and stresses at proximity regions. These regions are important, from the aspect of structural integrity, as, residual stress through thickness component of membrane stress has a dominant effect in estimating the stress intensity factor for a growing crack in the high tensile residual stress region, as investigated by [30], by the use of the stress decomposition technique [16]. Significant elevation in residual stress decomposed components of bending and membrane stress has been observed by [31] in repair welds.

3.1.2 Stress at weld center

Stresses measured at 2 mm depths in the center of weld A for all proximity distances were found to be generally less in magnitude when compared with the center of weld B, due to the weld pass sequence effect and the high heat

input of the TIG welding process (lower rate of cooling), as observed by [32] for plate butt welds. At the center of weld A, for 15 mm WP at 4 and 6 mm depths, a decrease in axial residual stress from 38 ± 18 MPa to compressive 21 ± 18 MPa was observed, in contrast to the 5 mm proximity distance, where an increase in axial tensile residual stress value from 132 ± 18 to 221 ± 18 MPa was found, as shown in Fig. 6b and c, respectively. For the 10 mm proximity distance, an increase in values from 96 ± 18 to 126 ± 18 MPa was found, when measured at 4 and 6 mm depths at the center of weld A.

In the 15 mm WP case, the minimum interaction is present between proximity welds; hence, the axial residual stresses observed at the center of weld B at 2 mm depth from the top are found to be higher than the 5 and 10 mm proximities. However, the axial tensile residual stress magnitudes for 5 and 10 mm proximities were found to be higher at 4 and 6 mm depths, in contrast to 15 mm WP. The most dominant effect is seen for 5 mm WP, where stresses increased from 69 ± 18 to 371 ± 18 MPa for 2 and 6 mm depths, respectively. Stresses measured at the center of weld B, at 6 mm from the top, were found to be give an average value of more than 355 MPa, which is higher than the yield strength of the parent metal for 5 and 10 mm proximity distances, in contrast to 15 mm WP. This behavior can be attributed to the complex interaction between the rate of cooling per unit weld pass volume of weld B and the high restraint present between 5 and 10 mm proximity welds.

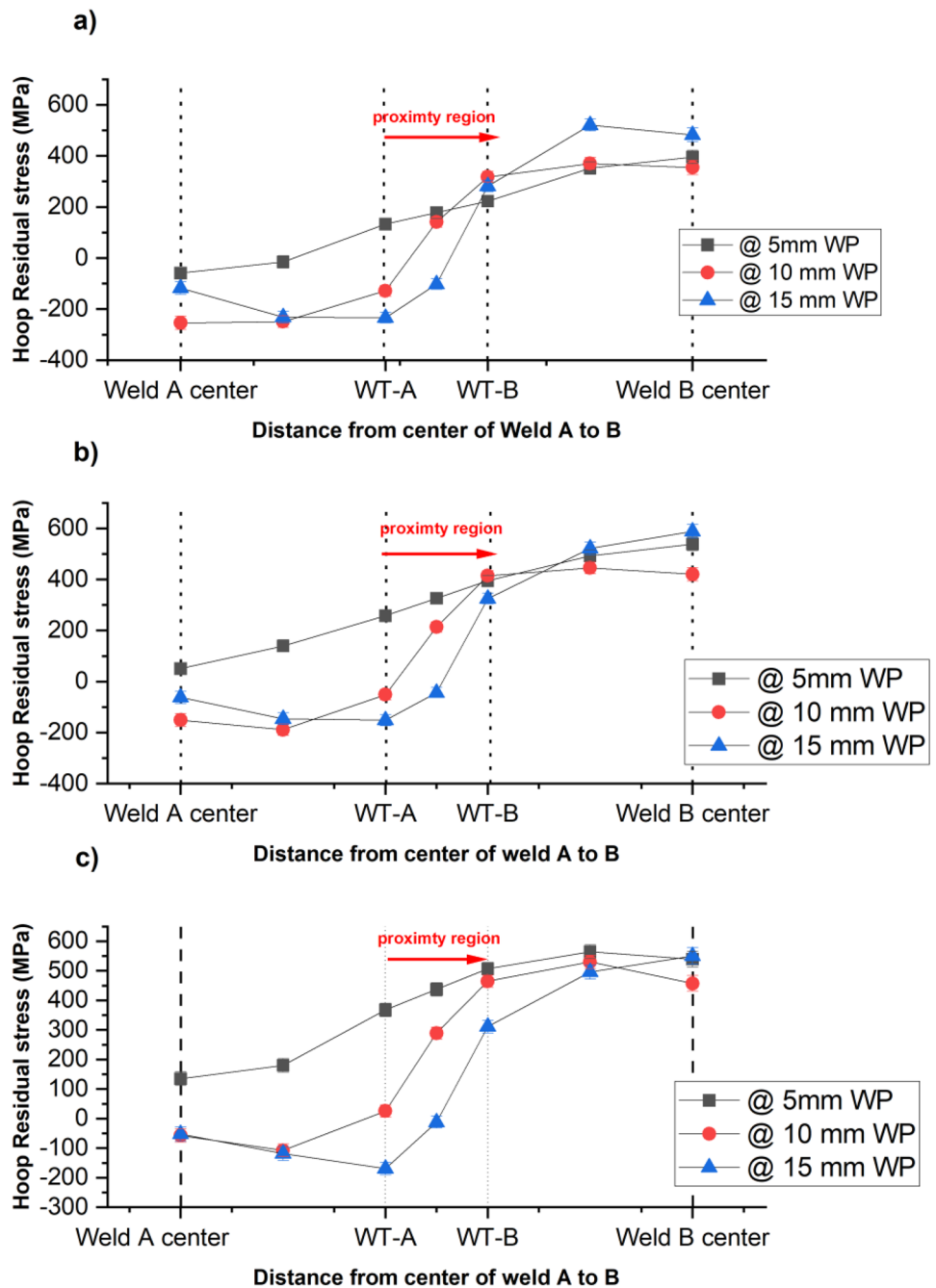
3.2 Hoop residual stress: longitudinal to weld direction

The maximum tensile residual stresses measured in the hoop direction, i.e., longitudinal, or parallel to the weld, are generally found to be higher in magnitude when compared with axial stresses, as reported by other authors [32, 33]. As shown in Fig. 7, hoop residual stresses for 5, 10, and 15 mm WP are presented when measured at different depths (i.e., 2, 4, and 6 mm) from the top of the weld cap into the thickness, starting from the center of weld A towards B.

3.2.1 Stress at proximity regions

The values of hoop stresses measured at 2, 4, and 6 mm depths were found to be highest for the 5-mm proximity distance, when compared with the 10 and 15 mm proximity distances. At 2 mm depth from the weld cap into the thickness, a tensile hoop stress value of 177 ± 18 MPa was found for the 5 mm proximity distance, when compared with the 10 and 15 mm proximity distances, where values of 141 ± 18 MPa and compressive 102 ± 18 MPa, respectively, were measured, as shown in Fig. 7a. The values measured at 2 mm depths close to WT for all proximity cases were less

Fig. 7 Hoop residual stress for WP_5 mm, WP_10 mm, WP_15 mm proximity distances at **a)** 2 mm (cap) **b)** 4 mm (mid thickness) **c)** 6 mm depth (root), level respectively



tensile in magnitude than for the 4 and 6 mm depths, due to the maximum interaction and tempering effect present between adjacent welds. The highest hoop stress values of 326 ± 18 MPa and 437 ± 18 MPa were found at 4 and 6 mm depths, respectively, for 5 mm proximity distance between adjacent welds, as shown in Fig. 7b and c, respectively. In the case of 10 and 15 mm WPs, due to the increasing distance between tapered weld grooves along the thickness, hoop stresses' values were found to be low in magnitude in contrast to the 5 mm WP.

At 10 mm proximity distance, stress values measured at the proximity region were less tensile in nature, with magnitudes of 213 ± 18 MPa and 290 ± 18 MPa at 4 and 6 mm depths, respectively; however, these were still lower than the 5 mm proximity distance, due to the lesser restraining effect of adjacent weld B. As 15 mm is the maximum distance used as proximity in this study, the values found between adjacent weld toes were found to be compressive in nature. This corroborates the fact that residual stresses are self-balanced internal stresses, where tensile stresses found at the weld

center are balanced by compressive stresses [28] found generally in the heat-affected zone (HAZ) of girth welds. This trend was also noted in axial residual stress at the proximity region, as high tensile stresses at weld B's center are balanced by less tensile or converging towards compressive stresses for the 15-mm proximity case, at all depths.

3.2.2 Stress at weld center

Hoop stresses measured at the center of weld A were found to be considerably lower in magnitude than those measured at the center of weld B at all depths and WP distances. However, at the center of weld B, hoop stresses are more tensile in nature, with high magnitude. Stresses found at the center of weld B were found to be in the range of minimum 355 ± 18 MPa and maximum 590 ± 18 MPa in magnitude, for all proximity distances, which was found to be more than the yield strength values of parent metal S355, used in this current study. With increasing depths, the magnitudes of hoop stresses at weld B center were found to be higher, due to through thickness stress gradient, without being affected by additional restraint caused by weld A, for all proximity distances. It was interesting to note that the stress value found at 6 mm depth of weld B center was higher than 590 MPa, as shown in Fig. 7c, which can be attributed to the following reasons: (a) tensile strength of the filler wire used for fabricating weld B, was found to be in the range of 530–680 MPa as reported in [21]; (b) not using proper diffraction elastic constants which might be varying along the weld and the depth of the weld due to crystallographic texture and also slight chemical heterogeneities; (c) the chemical composition of the filler wire is slightly different although the cut samples did not show significant variations in the lattice parameter, some chemical segregation might locally affect the measured lattice parameter; (d) possible porosity in the weld which would result in measurement pseudo-strains.

Hoop residual stresses measured at weld B's center for 5 mm WP were found to be increasing with increasing depths, due to the complex interaction between naturally developed hoop direction restraint and additional restraint caused by the minimum proximity distance for girth welds. Hoop stresses observed for the 5 mm proximity region in the center of weld B at 4 and 6 mm depths were found to be higher than axial residual stresses at the same locations, in agreement with the general trend, as reported by [32, 33] for plates and [34] for tubular girth welds. However, hoop residual stresses at the center of weld A, were found to be lower in magnitude than the corresponding axial stress components. This can be attributed to the complex interaction developed at weld A, due to different welding sequences and maximum restraint caused using two different heat inputs.

3.3 Radial residual stress: into the weld thickness

As shown in Fig. 8, radial residual stresses for 5, 10, and 15 mm WP are presented when measured at different depths (i.e., 2, 4, and 6 mm) from the top of the weld cap into the thickness, starting from the center of weld A towards B.

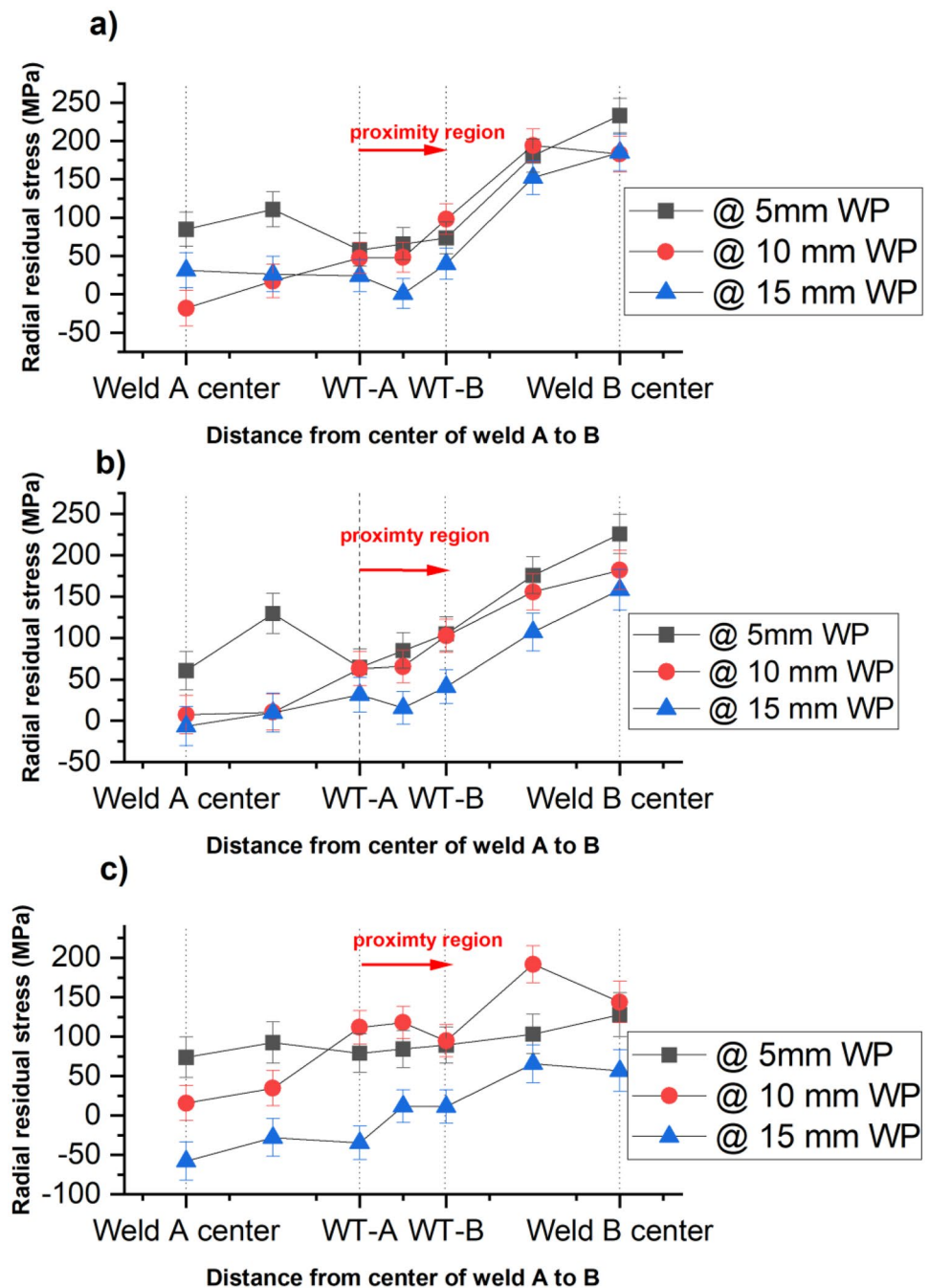
3.3.1 Stress at proximity regions

The values of radial stresses measured at 2, 4, and 6 mm depths were found to be generally lower in magnitude in contrast to axial and hoop components for all proximity distances. At 2 mm depth from the weld cap into the thickness, a tensile radial stress value of 65.3 ± 18 MPa was found for the 5 mm proximity distance, when compared with the 10 and 15 mm proximity distances, where values of 48 ± 18 MPa and compressive 8.75 ± 18 MPa, respectively, were measured, as shown in Fig. 8a. The values measured at 2 mm depths close to WT for all proximity cases were less tensile in magnitude than for the 4 and 6 mm depths, due to the maximum interaction and tempering effect present between adjacent welds. The highest radial stress values of 84 ± 18 MPa were found at 4 and 6 mm depths, respectively, for 5-mm proximity distance between adjacent welds, as shown in Fig. 8b and c, respectively. In the case of 15 mm WPs, due to the increasing distance between tapered weld grooves along the thickness, radial stresses' values were found to be low in magnitude in contrast to the 5 mm WP. At 10 mm proximity distance, stress values measured at the proximity region were less tensile in nature, with magnitudes of 65 ± 18 MPa and 117 ± 18 MPa at 4 and 6 mm depths, respectively; however, these were less than the 5 mm proximity for 4 mm depth and higher at 6 mm depth that can be attributed to complex restraining effect of adjacent weld B. As 15 mm is the maximum distance used as proximity in this study, the values found between adjacent weld toes were found to be compressive in nature. It should be noted that radial stresses become less important for estimating crack propagation direction in tubular restrained joints in contrast to its axial component [20].

3.3.2 Stress at weld center

Radial stresses measured at the center of weld A were found to be considerably lower in magnitude than those measured at the center of weld B at all depths and WP distances. However, at the center of weld B, radial stresses are more tensile in nature, with high magnitude but less than its respective axial and hoop components. Stresses found at the center of weld B were found to be in the range of minimum 56 ± 18 MPa and maximum 233 ± 18 MPa in magnitude, for all proximity distances, which was found

Fig. 8 Radial residual stress for WP_5 mm, WP_10 mm, WP_15 mm proximity distances at a) 2 mm (cap) b) 4 mm (mid thickness) c) 6 mm depth (root), level respectively



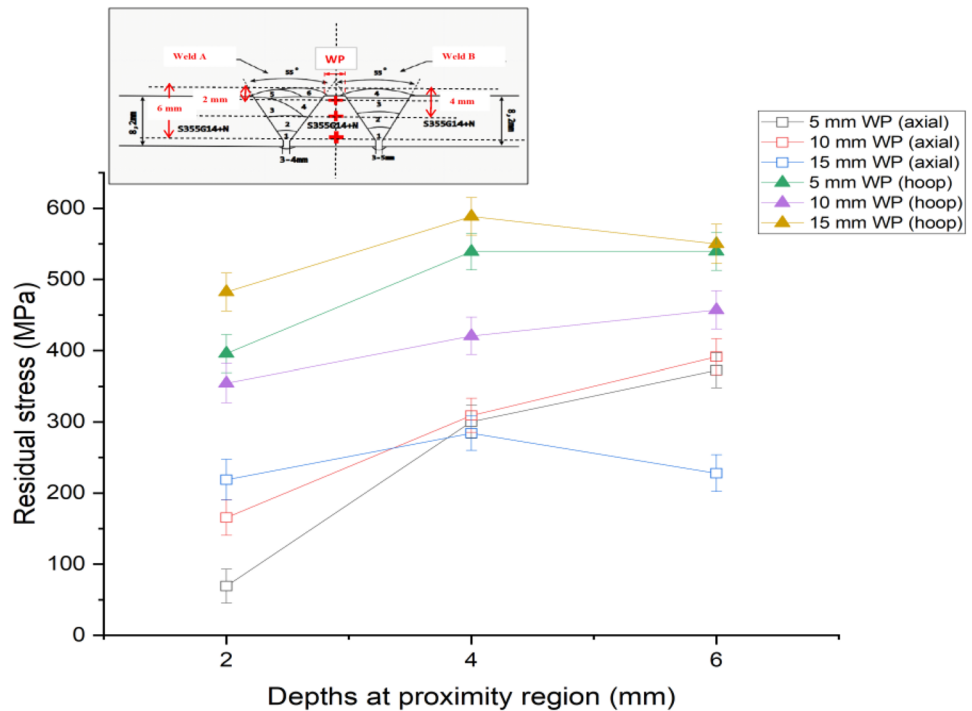
to be less than the yield strength values of parent metal S355, used in this current study.

3.4 Through thickness axial and hoop residual stress at proximity region

Residual stresses measured in the through thickness direction displayed an increasing trend when measured from the outside to the inside of the pipe at the proximity region for different depths, as shown in Fig. 9. When measured at the proximity region for 5 mm WP, residual stresses were

found to have values equal to and higher than the yield strength of the parent material in the axial and hoop directions, respectively, at 6 mm depth. This region is important for maintaining the structural integrity of proximity girth welds. Residual stresses at the proximity region in through thickness were found to be maximum for 5 mm WP, in contrast to the 10 and 15 mm cases, due to the presence of maximum restraint and complex interaction between the high rate of cooling at 6 mm depths. Beyond mid-thickness, i.e., 4 mm, the stress gradient effect is more pronounced when compared with 2 mm depths, having

Fig. 9 Through thickness axial and hoop residual stress at proximity region of WP_5 mm, WP_10 mm, WP_15 mm proximity distances at 2, 4, and 6 mm depths



compression on the outside and tension on the inside of the pipe, as discussed by [29, 35], for weld toe regions of thin girth welds. In principle, the general trend of hoop stresses being higher than axial stresses was found relevant at the proximity regions used in this study.

4 Conclusion

In this work, welding-induced residual stresses were measured experimentally at the proximity region of tubular girth welded samples of S355 steel, with 5, 10, and 15 mm minimum distances maintained between their weld toes, by the use of the neutron diffraction technique on the POLDI time-of-flight diffractometer at the Paul Scherrer Institute. The welds placed at proximity were welded with two different welding processes, simulating the practical situation of a repair weld (weld B) being welded adjacent to an existing weld (weld A), generally fabricated during repair/replacement procedures on piping, pipelines, and the high restraint weld geometry of offshore jacket structures. The neutron diffraction method is a powerful technique for measuring welding-induced residual stresses in the bulk of the material. The findings of this study enable practitioners to take remedial actions to minimize the residual stresses developed in girth welds fabricated at proximity. Also, the findings enable us to derive technical justification for maintaining a minimum distance and developing welding procedure for welds fabricated at proximity. The key findings of this experimental study are as follows:

- Axial residual stresses were found to be maximum at the proximity region of 5 mm WP, when measured at 6 mm depth from the top for line scan measurements, displaying global bending behavior, i.e., compression on the outside and tension on the inside surface of the pipe.
- Tensile axial residual stresses for 5 mm WP at 6 mm depth, when measured at the proximity region, were found to be more than the yield strength of the parent material used in this study. This is important while performing weld integrity assessments on the girth welds of tubular structures, due to the dominant axial loading conditions present in tubular welded structures.
- Hoop residual stresses for 5 mm WP, when measured at the proximity region, were found to increase with deeper depths of measurement and exceeding the value of the yield strength of the parent material used in this study at 6 mm depth from the top of the weld cap into the thickness.
- Hoop residual stresses measured at the center of weld B were found to be the highest in magnitude at 6 mm depth, exceeding the value of the yield strength of the material for all proximity distances, due to the complex interaction developed between the natural hoop direction restraint present in girth welds and the restraint developed due to minimum proximity distance between adjacent welds.
- Stresses measured (both axial and hoop) at the center of weld A were mainly low in magnitude (less tensile), due to the high heat input of TIG welding, generating lower cooling rates, followed by the welding sequence

of weld B (FCAW – low heat input process), which was welded after the completion of weld A. The maximum effect of tempering was seen at 2 mm depth from the top of the center of the weld for all WPs.

- The most deleterious effect was observed at the proximity region location for the 5 mm proximity distance at the inner diameter of the pipe, as the maximum stress values of hoop and axial tensions were recorded.
- Radial stresses observed for all proximity distances were low in magnitude in contrast to hoop and axial components.
- The maximum proximity distance of 15 mm used in this study did not seem to indicate any deleterious effect between adjacent welds and followed the general residual stresses principle of high tension being balanced by compression at the weld center and HAZ or proximity region.

Hence, stress relaxation procedures like heat treatment can be introduced with the utmost care, as an important part of welding qualification procedures for proximity welds, when the minimum distance between adjacent weld toes is less than one thickness of the joining structural member. In future, the authors plan to measure residual stress distribution through other NDT techniques like XRD etc. and compare them with numerical thermo-mechanical numerical models in finite element for various distances on proximity welds.

Abbreviations λ : Wavelength; n : An integer; d : Spacing between planes of atomic lattice under strain; hkl: Miller indices defining lattice plane; d_o : Spacing between planes of atomic lattice in strain-free state; θ : Angle between incident and scattering beams; ϵ : Strain; σ_x : Residual stress in axial direction; σ_y : Residual stress in hoop direction; σ_z : Residual stress in radial direction; ϵ_x : Residual strain in axial direction; ϵ_y : Residual strain in hoop direction; ϵ_z : Residual strain in radial direction; E : Young's modulus; μ : Poisson's ratio

Acknowledgements We would like to acknowledge the support of M/s Rosenberg Worley, Stavanger, Norway, and Jan-Tore Jakobsen, lab engineer at University of Stavanger, Norway, for their support in the fabrication of samples. We would also like to acknowledge the support of the Norwegian McNeutron program, under which three days' beam time was allotted at PSI, Switzerland, and the University of Stavanger, Norway UiSScatt program, for providing financial assistance for this study. The research is fully funded by the Norwegian Ministry of Education (Internal PhD project No. IN-12168). This work has been carried out as part of a PhD research project, performed at the University of Stavanger, Norway. Jan Capek gratefully acknowledges financial support from the Strategic Focus Area Advanced Manufacturing (SFA-AM) initiative of the ETH Board.

Author contribution Sachin Bhardwaj: conceptualization, experimentation, investigation, methodology, visualization, writing – original draft, writing – review and editing, data analysis; R.M. Chandima Ratnayake: conceptualization, formal analysis, review and editing, funding acquisition, project administration, supervision; Efthymios Polatidis: experimentation, data analysis; Jan Capek: experimentation, data analysis.

Funding Open access funding provided by University Of Stavanger. The research is fully funded by the Norwegian Ministry of Education (Internal PhD project No. IN-12168). This work has been carried out as part of a PhD research project, performed at the University of Stavanger, Norway.

Data availability All data generated and analyzed during this research are included in this published article.

Code availability Not applicable.

Declarations

Ethics approval Not applicable.

Consent to participate Not applicable.

Consent for publication Not applicable.

Conflict of interest The authors declare no competing interests.

Open Access This article is licensed under a Creative Commons Attribution 4.0 International License, which permits use, sharing, adaptation, distribution and reproduction in any medium or format, as long as you give appropriate credit to the original author(s) and the source, provide a link to the Creative Commons licence, and indicate if changes were made. The images or other third party material in this article are included in the article's Creative Commons licence, unless indicated otherwise in a credit line to the material. If material is not included in the article's Creative Commons licence and your intended use is not permitted by statutory regulation or exceeds the permitted use, you will need to obtain permission directly from the copyright holder. To view a copy of this licence, visit <http://creativecommons.org/licenses/by/4.0/>.

References

1. Bhardwaj S, Ratnayake RC (2020) Residual stress estimation in defect assessment procedures at weld toe and away locations on girth welds: review of key parameters. *Theoretical and Applied Fracture Mechanics*: p. 102848. <https://doi.org/10.1016/j.tafmec.2020.102848>
2. Larsson M, Larsson M, Ratnayake RM (2021) Experimental Investigation of weld joints manufactured at close proximity in S420 structural steel. in *Proceedings of 1st International Conference on Structural Damage Modelling and Assessment*. Singapore: Springer Singapore. https://doi.org/10.1007/978-981-15-9121-1_25
3. Bhardwaj S, Ratnayake RC (2020) Challenges due to welds fabricated at a close proximity on offshore structures, pipelines, and piping: state of the art. in *ASME 2020 39th International Conference on Ocean, Offshore and Arctic Engineering*. <https://doi.org/10.1115/OMAE2020-18586>
4. DNVGL-ST-0126 Standard (2018) Support structures for wind turbines. DNVGL
5. Bouchard PJ et al (2005) Measurement of the residual stresses in a stainless steel pipe girth weld containing long and short repairs. *Int J Press Vessels Pip* 82(4):299–310. <https://doi.org/10.1016/j.ijvp.2004.08.008>
6. Dong P, Zhang J, Bouchard PJ (2001) Effects of repair weld length on residual stress distribution. *J Pressure Vessel Technol* 124(1):74–80. <https://doi.org/10.1115/1.1429230>

7. George D, Smith DJ (2005) Through Thickness measurement of residual stresses in a stainless steel cylinder containing shallow and deep weld repairs. *Int J Press Vessels Pip* 82:279–287. <https://doi.org/10.1016/j.ijpvp.2004.08.006>
8. Lotsberg I (2016) *Fatigue design of marine structures*. Cambridge University Press, Cambridge
9. Link M (2021) Equinor: several factors behind faulty welds on Johan Castberg FPSO Hull. Available from: [https://www.marinelink.com/news/equinor-several-factors-behind-faulty-486965#.YH4FKi90m_8.linkedin\[cited 2021 29/09/2021\]](https://www.marinelink.com/news/equinor-several-factors-behind-faulty-486965#.YH4FKi90m_8.linkedin[cited%2021%2029/09/2021]);
10. Acevedo C, Drezet J-M, Nussbaumer A (2013) Numerical modelling and experimental investigation on welding residual stresses in large-scale tubular K-joints. *Fatigue Fract Eng Mater Struct* 36:177–185. <https://doi.org/10.1111/j.1460-2695.2012.01712.x>
11. Barsoum Z, Barsoum I (2009) Residual stress effects on fatigue life of welded structures using LEFM. *Eng Fail Anal* 16:449–467. <https://doi.org/10.1016/j.engfailanal.2008.06.017>
12. Bate SK et al (1998) A review of residual stress distributions in welded joints for the defect assessment of offshore structures. Offshore technology report. Vol. OTH 482. Sudbury: HSE Books
13. British Standard (2019) BS 7910 Guide to methods for assessing the acceptability of flaws in metallic structures: UK
14. American Petroleum Institute (2007) API RP 579–1/ASME FFS-1. Houston, TX: American Petroleum Institute; August 2007.: USA
15. British Energy Generation Ltd (2013) Procedure R6 revision 4, assessment of the integrity of structures containing defects. 2013: UK
16. Dong P et al (2014) On residual stress prescriptions for fitness for service assessment of pipe girth welds. *Int J Press Vessels Pip* 123–124:19–29. <https://doi.org/10.1016/j.ijpvp.2014.07.006>
17. Larsson M et al (2021) Experimental Residual stress investigation of weld joints fabricated at a close proximity in S420 structural steel. In *Proceedings of 1st International Conference on Structural Damage Modelling and Assessment*. Singapore: Springer Singapore. https://doi.org/10.1007/978-981-15-9121-1_26
18. Acevedo C, Nussbaumer A (2013) Effect of tensile residual stresses on fatigue crack growth and S-N curves in tubular joint in compression. *Int J Fatigue* 36:171–180. <https://doi.org/10.1016/j.ijfatigue.2011.07.013>
19. Larsson M, Larsson M, Ratnayake RM (2021) Investigation of fatigue strength behaviour in dual weld S420 Steel joints fabricated at a close proximity. In *Proceedings of 1st International Conference on Structural Damage Modelling and Assessment*. Singapore: Springer Singapore. https://doi.org/10.1007/978-981-15-9121-1_27
20. Acevedo C (2011) Influence of residual stresses on fatigue response of welded tubular K-joints. EPFL, Switzerland
21. Bhardwaj S, Ratnayake RMC (2022) Welding procedure qualification record (WPQR) for welds fabricated at proximity. *The International Journal of Advanced Manufacturing Technology*. <https://doi.org/10.1007/s00170-022-09022-5>
22. ENISO15614–1 Standard (2017) Specification and qualification of welding procedures for metallic materials — welding procedure test
23. Paradowska A et al (2006) Residual stress measurements by neutron diffraction in multi-bead welding. *Physica B* 385–386:890–893. <https://doi.org/10.1016/j.physb.2006.05.241>
24. Stuhr U et al (2005) Time-of-flight diffraction with multiple frame overlap Part II: the strain scanner POLDI at PSI. *Nucl Instrum Methods Phys Res, Sect A* 545:330–338. <https://doi.org/10.1016/j.nima.2005.01.321>
25. Arnold O et al (2014) Mantid—Data analysis and visualization package for neutron scattering and μ SR experiments. *Nucl Instrum Methods Phys Res, Sect A* 764:156–166. <https://doi.org/10.1016/j.nima.2014.07.029>
26. British Standards Institute (2019) Non-destructive testing — standard test method for determining residual stresses by neutron diffraction, in ISO 21432:2019: UK
27. Jacob A et al (2018) Residual stress measurements in offshore wind monopile weldments using neutron diffraction technique and contour method. *Theoret Appl Fract Mech* 96:418–427. <https://doi.org/10.1016/j.tafmec.2018.06.001>
28. Withers PJ, Bhadeshia HK, Withers PJ, Bhadeshia HK (2001) Residual stress. Part 1 – Measurement techniques. *Materials Science and Technology* 17(4): p. 355–365. <https://doi.org/10.1179/026708301101509980>
29. Song S, Dong P, Pei X (2015) A full-field residual stress estimation scheme for fitness-for-service assessment of pipe girth welds: Part I - Identification of key parameters. *Int J Press Vessels Pip* 126–127:58–70. <https://doi.org/10.1016/j.ijpvp.2015.01.002>
30. Dong P (2018) On repair weld residual stresses and significance to structural integrity. *Welding in the World* 62(2):351–362. <https://doi.org/10.1007/s40194-018-0554-1>
31. Song S, Dong P (2017) Residual stresses at weld repairs and effects of repair geometry. *Sci Technol Weld Joining* 22(4):265–277. <https://doi.org/10.1080/13621718.2016.1224544>
32. Alipooramirabad H et al (2015) Quantification of residual stresses in multi-pass welds using neutron diffraction. *J Mater Process Technol* 226:40–49. <https://doi.org/10.1016/j.jmatprotec.2015.07.002>
33. Kim S-H, Kim J-B, Lee W (2009) Numerical prediction and neutron diffraction measurement of the residual stresses for a modified 9Cr–1Mo steel weld. *J Mater Process Technol* 209:3905–3913. <https://doi.org/10.1016/j.jmatprotec.2008.09.012>
34. Stacey A et al (2000) Incorporation of residual stresses into the SINTAP defect assessment procedure. *Eng Fract Mech* 67:573–611
35. Bouchard PJ (2007) Validated residual stress profiles for fracture assessments of stainless steel pipe girth welds. *Int J Press Vessels Pip* 84(4):195–222. <https://doi.org/10.1016/j.ijpvp.2006.10.006>

Publisher's Note Springer Nature remains neutral with regard to jurisdictional claims in published maps and institutional affiliations.